Int. J. Heat Mass Transfer. Vol. 26, No. 9, pp. 1329–1338, 1983
Printed in Great Britain

0017-9310/83 $3.00 + 0.00
Pergamon Press Ltd.

INFLUENCE OF BUOYANCY FORCES AND THERMAL CONDUCTIVITY ON FLOW FIELD AND HEAT TRANSFER OF CIRCULAR CYLINDERS AT SMALL REYNOLDS NUMBER

BENGT SUNDÉN

Department of Applied Thermo and Fluid Dynamics, Chalmers University of Technology,
41296 Göteborg, Sweden

(*Received* 26 *June* 1982 *and in revised form* 4 *November* 1982)

Abstract—A numerical investigation of the influence of buoyancy forces and thermal conductivity ratio (k_s/k_f) on the flow field and heat transfer around circular cylinders is presented. The flow field and energy equations are solved under the conditions of continuity in temperature and heat flux at the fluid–solid interface. The buoyancy forces are taken into account by applying Boussinesq's approximation. Numerical results are given for Reynolds numbers in the range of $5 \leqslant Re \leqslant 40$, buoyancy parameters in the range of $-1 \leqslant Gr/Re^2 \leqslant 2$ and thermal conductivity ratios in the range of $0 \leqslant k_s/k_f \leqslant \infty$.

NOMENCLATURE

c_D drag coefficient
c_{D_0} drag coefficient for forced flow
D cylinder diameter or outer tube diameter
D_c diameter of the core region or inner tube diameter
f_1, f_2, f_3, f_4 functions in the asymptotic solutions of Ψ and ω
f_Ψ, f_ω, f_T functions in the numerical solution of Ψ, ω and T, respectively
f arbitrary function
Gr Grashof number, $g\beta(T'_c - T'_\infty)D^3/\nu^2$
g acceleration due to gravity
h step size in the numerical calculations
h' heat transfer coefficient
i, j integers
k_s thermal conductivity of the solid
k_f thermal conductivity of the fluid
Nu Nusselt number, $h'D/k_f$
Nu_0 Nusselt number for forced flow, $k_s/k_f = \infty$
n iteration number
Pr Prandtl number
r radial coordinate in the polar coordinate system
$R1, R2, R3$ relaxation parameters for the streamfunction, vorticity and temperature, respectively
Re Reynolds number, $U_\infty D/\nu$
T' temperature
T'_c temperature of the core region
T'_∞ temperature in the approaching stream at far distances
T dimensionless temperature, $(T' - T'_\infty)/(T'_c - T'_\infty)$
U_∞ velocity in the approaching stream

Greek symbols
α thermal diffusivity of the fluid
β coefficient of volumetric expansion
η coordinate in the (ξ, η) coordinate system
θ angle in the polar coordinate system
ν kinematic viscosity
ξ coordinate in the (ξ, η) coordinate system
ξ_∞ value of ξ at the outermost boundary
ξ_m value of ξ at the boundary next to ξ_∞
ρ density of the fluid
φ angle measured from the forward stagnation point
Ψ' streamfunction
Ψ dimensionless streamfunction
Ψ_0 uniform flow solution of Ψ
ω' vorticity
ω dimensionless vorticity

1. INTRODUCTION

HEAT transfer problems often involve a coupling of conduction in a solid and convection in an adjacent fluid. For situations where the buoyancy forces are of importance, the flow field will depend on the temperature and thereby on the ratio of the thermal conductivities (solid to fluid). For such problems, the flow field equations cannot be solved separately since these equations are coupled to the energy equation through the buoyancy forces. Further, the energy equations for the fluid and the solid have to be solved under the conditions of continuity in temperature and heat flux at the fluid–solid interface.

During recent years, studies concerning coupled conduction–convection heat transfer (or conjugate heat transfer) have been published with increasing frequency (e.g. ref. [1]).

The objective of the work reported below was to predict the combined influence of the buoyancy forces and the thermal conductivity ratio (solid to fluid) on the flow pattern around, and the heat transfer from, a circular cylinder with a heated core region in low Reynolds number flow. An infinite ratio of the thermal conductivity of the solid to that of the fluid gives the common case of a uniform temperature at the fluid–solid interface. The cases when the forced flow is in the direction of the gravity acceleration vector or in the direction opposite to it are considered. Numerical solutions have been obtained over a range of the Reynolds and Grashof numbers where neither the boundary layer assumptions nor the asymptotic matching techniques are applicable.

The forced flow field around a circular cylinder at low Reynolds number has been given much attention in the literature and the technique to calculate this flow field may be considered known.

Analyses of pure forced convection from circular cylinders at low Reynolds number have been given [2–6] while pure free or natural convection studies (for moderate Grashof numbers) have been presented [7, 8]. Nakai and Okazaki [9] investigated both pure forced and pure free convection. Analytical treatment of combined natural and forced convection has only been presented in a few papers [10, 11].

Experimental results and numerical calculations concerning mixed convection at high Reynolds and Grashof numbers (under boundary layer assumptions) have also been reported [12–22]. Some of these works will be commented on later, although they are not of direct interest for the present work. A review of works on heat transfer of circular cylinders has been presented by Morgan [23].

In the works quoted above the condition at the fluid–solid interface was either a uniform temperature or a uniform heat flux.

Coupled solid body conduction–forced convection for circular cylinders have been considered [1, 24, 25].

For the problem of coupled heat conduction within a solid circular cylinder to mixed convection in a fluid, only one set of results is available [26].

2. MATHEMATICAL FORMULATION

Consider the 2-dim. steady flow of an infinite stream of an incompressible viscous fluid past a long horizontal circular cylinder. The oncoming stream is uniform and has the velocity U_∞ and temperature T'_∞. The cylinder with the diameter D has a heated core region with a diameter D_c ($D_c \leqslant D$). The temperature of the core region is T'_c. The thermal conductivity of the solid material is k_s and that of the fluid is k_f. Heating by viscous dissipation is neglected and the kinematic viscosity and the coefficient of volumetric expansion are assumed to be constants throughout the fluid. The density of the fluid is assumed to vary with temperature and the resulting buoyancy forces are taken into account by applying Boussinesq's approximation.

In terms of the non-dimensional streamfunction Ψ, vorticity ω and temperature T, the governing equations are given by

flow field

$$\frac{\partial\Psi}{\partial\xi}\frac{\partial\omega}{\partial\eta}-\frac{\partial\Psi}{\partial\eta}\frac{\partial\omega}{\partial\xi}=\frac{2}{Re}\Delta\omega-\frac{1}{2}\frac{Gr}{Re^2}\times\pi\exp(\pi\xi)\left[\sin\pi(1-\eta)\frac{\partial T}{\partial\xi}-\cos\pi(1-\eta)\frac{\partial T}{\partial\eta}\right], \tag{1}$$

$$\Delta\Psi=-\omega\pi^2\exp(2\pi\xi), \tag{2}$$

convective heat transfer in the fluid

$$\frac{\partial\Psi}{\partial\xi}\frac{\partial T}{\partial\eta}-\frac{\partial\Psi}{\partial\eta}\frac{\partial T}{\partial\xi}=\frac{2}{Re\,Pr}\Delta T, \tag{3}$$

heat conduction in the solid

$$\Delta T=0, \tag{4}$$

where

$$\Delta=\partial^2/\partial\xi^2+\partial^2/\partial\eta^2.$$

The coordinates (ξ,η) are related to the polar coordinates (r,θ) by the relations

$$\xi=\frac{1}{\pi}\ln\frac{2r}{D}, \tag{5}$$

$$\eta=1-\frac{\theta}{\pi}. \tag{6}$$

The non-dimensional quantities in equations (1)–(4) are related to the dimensional quantities, indicated with a prime, as follows:

$$\Psi=2\Psi'/(U_\infty D);\quad \omega=\omega' D/(2U_\infty);$$
$$T=(T'-T'_\infty)/(T'_c-T'_\infty).$$

The dimensionless numbers in equations (1) and (3) are defined as

$$Re=U_\infty D/\nu;\quad Gr=g\beta(T'_c-T'_\infty)D^3/\nu^2;$$
$$Pr=\nu/\alpha=\mu c_p/k_f.$$

The Grashof number, Gr, is taken as positive when the forced flow is opposite to the gravity direction and negative when the forced flow is in the direction of the gravity vector.

Equations (1)–(4) are to be solved with respect to the following boundary conditions:

$$\xi\leqslant\frac{1}{\pi}\ln\frac{D_c}{D}:\quad T=1, \tag{7}$$

$$\xi=0\ \text{(fluid–solid interface)}:\quad \frac{\partial\Psi}{\partial\xi}=\frac{\partial\Psi}{\partial\eta}=0, \tag{8}$$

$$T_{\text{convection}}=T_{\text{conduction}}, \tag{9}$$

$$k_f\left(\frac{\partial T}{\partial\xi}\right)_{\text{fluid}}=k_s\left(\frac{\partial T}{\partial\xi}\right)_{\text{solid}}, \tag{10}$$

$$\xi\to\infty:\quad \Psi\to\exp(\pi\xi)\sin\pi\eta, \tag{11}$$

$$\omega, T \to 0. \quad (12)$$

Equation (8) expresses the no-slip boundary condition and equations (9) and (10) represent the conditions of continuity in temperature and heat flux, respectively. In equations (11) and (12) the approach to the uniform far field conditions is expressed.

The present investigation has been performed for Reynolds numbers in the range of $5 \leqslant Re \leqslant 40$, $-1 \leqslant Gr/Re^2 \leqslant 2$, $D_c/D \leqslant 1$ and $0 \leqslant k_s/k_f \leqslant \infty$, thereby using the further assumption of symmetry around the stagnation lines which has been shown to be a reasonable approximation in several experiments [8, 27, 28].

The present study is of interest in hot-wire anemometry, especially at low flow velocities when the cooling of the wire may be affected by both natural and forced convection. In the field of heat exchanger design, the study is applicable to situations where the fluid on the tubeside is a liquid with a very high heat transfer coefficient so that the inside tubewall has the same temperature as the fluid. Applications may also be found in the rating of electrical conductors.

3. NUMERICAL SOLUTION PROCEDURE

Finite difference equations

The governing equations are solved by using second-order finite difference approximations. On the (ξ, η) plane, a uniform grid with the same spacing h in both the coordinate directions is placed. In the physical plane, smaller meshes result near the cylinder surface and larger ones are found far from the body.

The finite difference equations of Ψ, ω and T are solved iteratively by a relaxation technique thereby using iterations in alternating directions. The following principal finite-difference equations are used:

$$\Psi_{i,j}^{n+1} = (1-R1)\Psi_{i,j}^{n} + R1 f_\Psi(\Psi_{i\pm1,j}, \Psi_{i,j\pm1}, \omega_{i,j}), \quad (13)$$

$$\omega_{i,j}^{n+1} = (1-R2)\omega_{i,j}^{n} + R2 f_\omega(\Psi_{i\pm1,j}, \Psi_{i,j\pm1}, \omega_{i\pm1,j}, \omega_{i,j\pm1}, T_{i\pm1,j}, T_{i,j\pm1}, Gr/Re^2, Re), \quad (14)$$

$$T_{i,j}^{n+1} = (1-R3)T_{i,j}^{n} + R3 f_T(\Psi_{i\pm1,j}, \Psi_{i,j\pm1}, T_{i\pm1,j}, T_{i,j\pm1}, Re\,Pr). \quad (15)$$

In equations (13)–(15), n is the number of iterations and $R1$, $R2$ and $R3$ the relaxation parameters. In the functions f_Ψ, f_ω and f_T, the latest values of the variables are always used. The grid notations in the η and ξ directions are given by i and j, respectively.

The relaxation parameters $R1$ and $R2$ are primarily dependent on the Reynolds number Re and the ratio Gr/Re^2 (ratio of buoyancy forces to inertia forces). With increasing Reynolds number, $R1$ and especially $R2$ must be diminished and under-relaxation is commonly necessary. On the other hand, at a constant Reynolds number and if the value of Gr/Re^2 is positive (i.e. if the forced flow is opposite to the gravity vector or it is a bottom to top problem) the relaxation parameters can be chosen higher than those for the corresponding forced flow and thus fewer iterations are needed to achieve a given convergence criterion. On the other hand, if Gr/Re^2 is negative (top to bottom problem) the numerical values of the relaxation parameters must be chosen smaller than those for the forced flow resulting in a poorer convergence rate.

The relaxation parameter $R3$ in equation (15) is for the convective heat transfer field depending on $Re\,Pr$. At a constant Reynolds number, $R3$ must be much smaller than unity for high Pr number fluids while for fluids with a low Pr number, values of $R3$ larger than unity can be used. For the conductive heat transfer field (within the solid) the optimal relaxation parameter for the Laplacian equation is always applied.

Boundary conditions at the fluid–solid interface

The streamfunction Ψ is set equal to zero along the fluid–solid interface in accord with equation (8). The values of the vorticity ω at the interface is calculated from equation (2) and the condition (8). The following second-order formula is used:

$$\omega(0,\eta) = \frac{7\Psi(0,\eta) - 8\Psi(h,\eta) + \Psi(2h,\eta)}{2\pi^2 h^2}. \quad (16)$$

The temperature distribution at the interface is found by a direct finite difference approximation of the conditions (9) and (10). The following second-order formula is used:

$$T(0,\eta) = \frac{T(-h,\eta) + (k_f/k_s)T(h,\eta)}{1 + (k_f/k_s)}. \quad (17)$$

As is evident from equations (16) and (17), the values of $\omega(0,\eta)$ and $T(0,\eta)$ are obtained as part of the numerical solution.

Boundary conditions due to symmetry

The flow and temperature fields are assumed to be symmetric around the stagnation lines as outlined above. This requires the following conditions to be satisfied:

$$\begin{aligned} &\eta = 0: \quad \frac{\partial \Psi}{\partial \xi} = 0, \quad \omega = 0, \quad \frac{\partial T}{\partial \eta} = 0. \\ &\eta = 1: \end{aligned} \quad (18)$$

The streamfunction is set equal to zero along the stagnation lines according to the condition in (18) and the interface value. A second-order approximation to the temperature gradient condition in (18) is found by inserting extra grid lines at $\eta = -h$ and $\eta = 1+h$.

Far field boundary conditions

One major problem when dealing with the flow around circular cylinders is the treatment of the boundary conditions at far distances. For a practical reason, the calculation domain must be cut off at some finite distance from the fluid–solid interface, say $\xi_\infty = (1/\pi)\ln(2r/D)_\infty$. An application of the uniform stream conditions [equations (11) and (12)] at finite distances from the cylinder surface is not so satisfactory because of the slow decay of the flow in the wake. If

equations (11) and (12) are applied, the drag coefficient is found to vary largely with ξ_∞ and the value is too high when compared to experiments. Correspondingly the temperature field becomes inaccurate. In order to complete numerical solutions with reasonable computing times but still obtaining accurate results it is necessary to adjust the far field conditions.

Since the present investigation is dealing with steady flows at moderate Reynolds numbers the asymptotic expression for Ψ and ω derived by Imai [29] can be employed. In this work the first two terms in those expressions are used. The following principal formulas then apply:

$$\Psi(\xi_\infty,\eta) = \Psi_0(\xi_\infty,\eta)+c_D f_1(\xi_\infty,\eta,Re)+c_D^2 f_2(\xi_\infty,\eta,Re), \tag{19}$$

$$\omega(\xi_\infty,\eta) = c_D f_3(\xi_\infty,\eta,Re)+c_D^2 f_4(\xi_\infty,\eta,Re) \tag{20}$$

where Ψ_0 is the uniform flow solution given in equation (11). The functions f_1, f_2, f_3 and f_4 can be found in ref. [1].

It is important to note that formulas (19) and (20) depend on the drag coefficient and thus the far field values of Ψ and ω are found as part of the numerical solution.

Equations (19) and (20) have been used before [24–26, 30–32]. Parts of equations (19) and (20) have also been used [6, 33–36]. The importance of using proper far field conditions was pointed out in these works.

For the temperature far field, the Oseen solution of the energy equation (3) is applied and the following relationship is used:

$$\frac{T(\xi_\infty,\eta)}{T(\xi_m,\eta)} = \exp\{[\cos\pi(1-\eta)-1](X_\infty-X_m)-(\xi_\infty-\xi_m)\pi/2\} \tag{21}$$

where ξ_m is the grid line situated just inside to ξ_∞. X is defined as

$$X = \frac{Re\,Pr}{4}\exp(\pi\xi). \tag{22}$$

The expression (21) is essentially one used previously [1, 2, 6, 24–26].

Modifications of both the flow and temperature far field conditions through the equations (19)–(22) have only been considered by Sundén [1, 24–26]. Apelt and Ledwich [6] used equation (21) but did not correct the streamfunction and only used the first term in equation (20). This was in a study concerning heat transfer in unsteady forced flow.

Another possible way to get proper approximations of the far field is to assume that the derivatives of the streamfunction, vorticity and temperature are equal to the derivatives of the uniform flow solution. We then have

$$\left(\frac{\partial\Psi}{\partial\xi}\right)_{\xi_\infty} = \pi\exp(\pi\xi_\infty)\sin\pi(1-\eta), \tag{23}$$

$$\left(\frac{\partial\omega}{\partial\xi}\right)_{\xi_\infty} = 0, \tag{24}$$

$$\left(\frac{\partial T}{\partial\xi}\right)_{\xi_\infty} = 0. \tag{25}$$

The expressions (23)–(25) are very easy to use in the calculations since there is no need for the drag coefficient as in equations (19) and (20). The conditions (23) and (24) have been found to work reasonably well and some of the results will be commented on later.

In a study basically concerned with computation of steady flows at high Reynolds number, Fornberg [35] also used conditions equivalent to those in (23) and (24) with successful and consistent results.

In the literature, mixed conditions, connecting the functions and their first derivatives, have also been presented [35, 36]. These methods will not be considered further in this paper.

Drag and heat transfer coefficients

The drag coefficient c_D is calculated at the fluid–solid interface and the following formula can be derived:

$$c_D = \frac{4}{Re}\int_0^1\left(\frac{\partial\omega}{\partial\xi}\right)_0\sin\pi\eta\,d\eta - \frac{4\pi}{Re}\int_0^1\omega(0,\eta)\sin\pi\eta\,d\eta - \frac{Gr}{Re^2}\pi\int_0^1 T(0,\eta)\sin^2\pi(1-\eta)\,d\eta. \tag{26}$$

The film heat transfer coefficient is defined with respect to the temperature difference $T'_c - T'_\infty$ and for the Nusselt number we have

$$Nu = \frac{2}{\pi}\left(\frac{\partial T}{\partial\xi}\right)_{\xi=0}. \tag{27}$$

The first derivatives in equations (26) and (27) are calculated with the formula

$$\left(\frac{\partial f}{\partial\xi}\right)_{\xi=0} = \frac{4f(h,\eta)-f(2h,\eta)-3f(0,\eta)}{2h} \tag{28}$$

where f is either ω or T. The truncation error in equation (28) is of $O(h^2)$.

Convergence and accuracy

The numerical calculations have been carried out on IBM 370/3031 and 3033N computers in single precision.

When the relative increases or decreases in the drag coefficient, the local Nusselt numbers and interface temperatures were less than 10^{-5}, the iterative procedure was terminated.

In order to establish the accuracy in the numerical solutions a number of test calculations were performed. These were mainly for forced convection but the conclusions are supposed to be valid also for combined forced and free convection.

So for instance a careful study of the influence of the step size was carried out. The most proper value was found to be $h = 0.02$. The reasons for this choice can be found elsewhere [1].

By using Imai's asymptotic solution including the first two terms [equations (19) and (20)], the numerically calculated results ideally should be independent of the position of the outer boundary, that is, the value of ξ_∞ or $(2r/D)_\infty$. In the present work, $(2r/D)_\infty$ was varied in the range of 14–29.75 and from the calculated results an extrapolation to $(2r/D)_\infty = \infty$ was carried out. The results so obtained were almost identical to the results of Fornberg [35] and Dennis [36]. It was also found that the drag coefficient calculated for $(2r/D)_\infty = 14$ was 1.5% too high at $Re = 20$ and 3% too high at $Re = 40$.

The effect of different values of ξ_∞ or $(2r/D)_\infty$ on the heat transfer when using equations (19)–(22) for the far field was found to be less than 0.5%.

If only the first correction terms in equations (19) and (20) were used, the drag coefficient for $(2r/D)_\infty = 14$ at $Re = 20$ was 5.8% too high while at $Re = 40$ the drag coefficient was 6.8% too high.

Test calculations with the far field conditions (23) and (24) were also carried out. Again the conditions were applied at distances in the range of $14 \leqslant (2r/D)_\infty \leqslant 29.75$. At $Re = 20$, the drag coefficients for $(2r/D)_\infty = 14$ and $(2r/D)_\infty = 29.75$ were 2.8% and 0.8%, respectively, below the true value at $(2r/D)_\infty = \infty$. From these test results and the results of Fornberg [35] it is concluded that the simple conditions (23) and (24) are effective.

If proper far field conditions are used for the flow field, it has been found that the condition for the temperature field at far distances is not critical if the interest of the heat transfer study is focused on the region closest to the fluid–solid interface. This might be so because the heat transfer is primarily dominated by wall conditions.

The results which will be presented in this paper are those obtained for $(2r/D)_\infty = 14$ with a step size $h = 0.02$. The far field conditions (19)–(22) are used. The absolute accuracy can then be estimated from what has been stated above. Mostly however, only relative results will be given.

4. RESULTS AND DISCUSSION

All the results presented in this paper are for a Prandtl number $Pr = 0.72$.

Figure 1 shows the streamlines at $Re = 20$, $D_c/D = 0.11$ and $k_s/k_f = 4$ for different strengths of the buoyancy forces. If we take $Gr/Re^2 = 0$ (pure forced flow) as the standard case we can see that a positive value of Gr/Re^2 (favourable gravity effect) makes the recirculating flow region on the backward side of the cylinder smaller and thus the separation point is moved towards the rear stagnation point. The wake length is also much decreased. Above a certain positive value of Gr/Re^2 no separation occurs. On the other hand, if Gr/Re^2 is negative (adverse gravity effect) the separation point moves towards the forward stagnation point and the wake lengthens and the separated region occupies more space and the streamlines are displaced from the body. For larger negative values of Gr/Re^2 the flow region close to the cylinder surface will be recirculating and the wake is extended over a major region on the rear side.

Besides the important physical effect of the buoyancy forces on the flow pattern also different strengths of buoyancy forces affects the numerical procedure. It should be pointed out that it is very difficult to obtain fully converged solutions for large negative values of Gr/Re^2.

In Fig. 2 the effect of the buoyancy forces on the vorticity field is shown. At $Gr/Re^2 = 0$ the intense generation of vorticity on the upstream surface and its spread downstream are clearly evident. For high positive values of Gr/Re^2, the vorticity is confined to a region close to the surface and high gradients on both the upstream and downstream sides exist. This seems to be in agreement with the appearance of a small wake or no wake at all. For negative values of Gr/Re^2 the downstream spread of the vorticity is increased.

The influence of the thermal conductivity ratio k_s/k_f on the flow pattern is shown in Fig. 3 for $Re = 20$, $Gr/Re^2 = 0.3$ and $D_c/D = 0.11$. By increasing k_s/k_f the

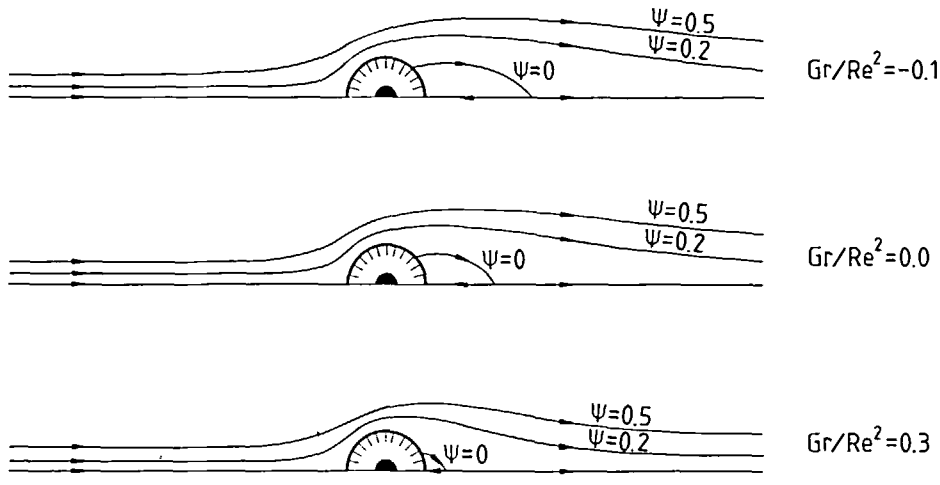

FIG. 1. Influence of Gr/Re^2 on the flow field (streamlines). $Re = 20$, $k_s/k_f = 4$, $D_c/D = 0.11$.

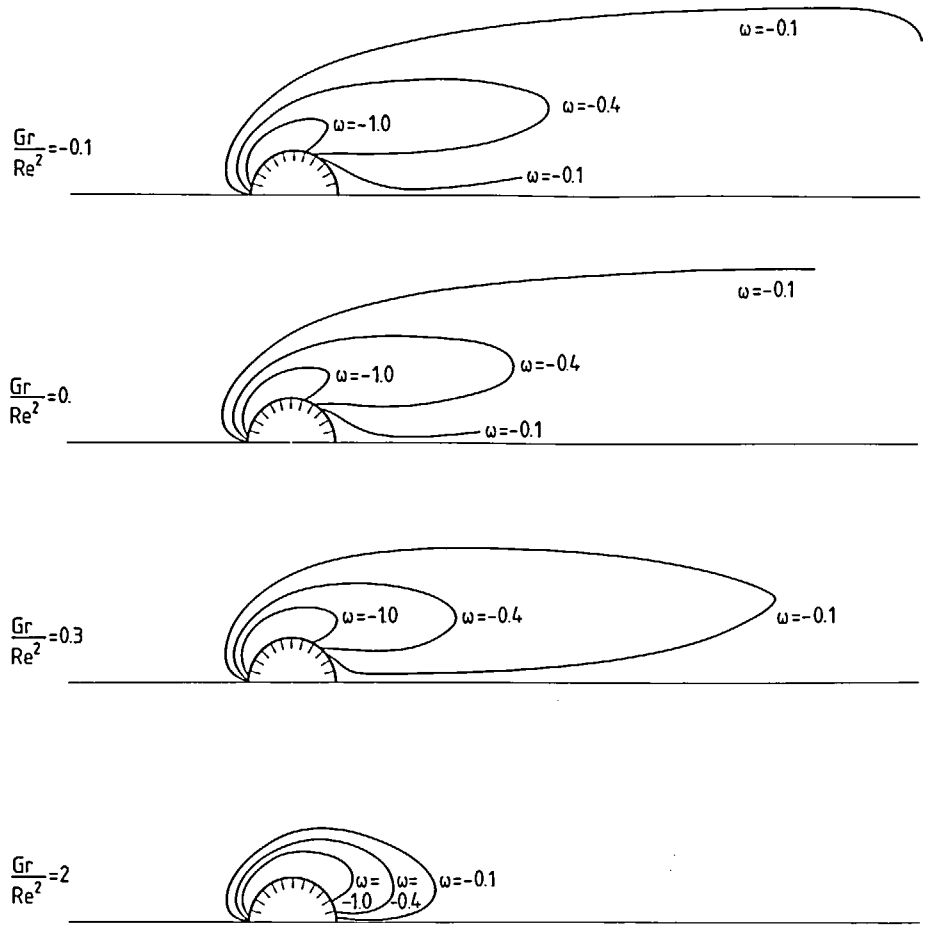

FIG. 2. Influence of the buoyancy forces (Gr/Re^2) on the vorticity field. $Re = 20$, $k_s/k_f = 4$ and $D_c/D = 0.11$.

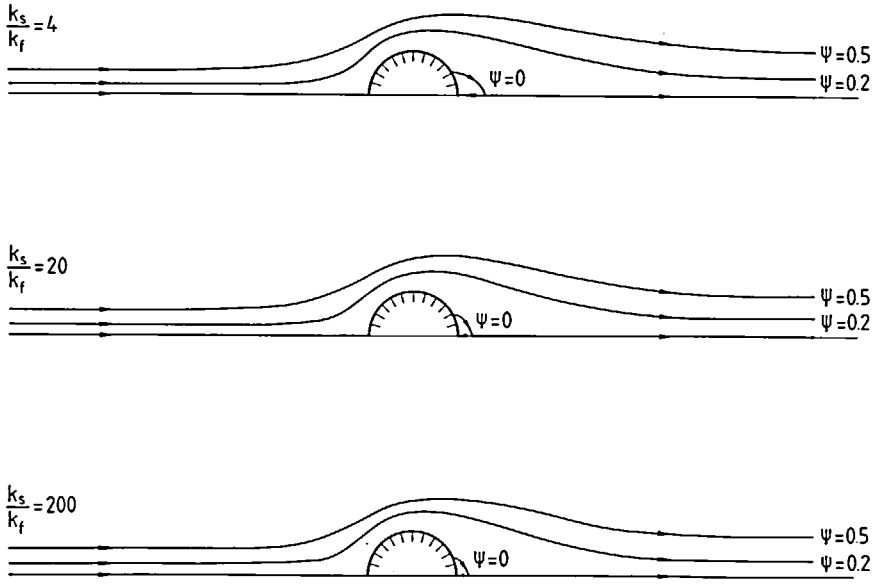

FIG. 3. Influence of the thermal conductivity ratio on the streamlines. $Re = 20$, $Gr/Re^2 = 0.3$ and $D_c/D = 0.11$.

insulation of the core region becomes weaker and thus the temperature driven force on the fluid will be stronger and in Fig. 3 we see what happens for a favourable gravity effect. The wake region on the rear side becomes smaller and smaller. If $Gr/Re^2 = 0$ there is no effect of k_s/k_f on the flow pattern. For negative values of Gr/Re^2, reversed results appear with increasing k_s/k_f. However, as is evident when comparing the results in Fig. 1 with those in Fig. 3, the parameter Gr/Re^2 has a stronger effect than the thermal conductivity ratio.

As will be seen later on, also the temperature field and thus the heat transfer are affected by Gr/Re^2 and k_s/k_f.

Calculations for several other values of the parameters Re, Gr/Re^2 and D_c/D than those shown in Figs. 1–3 have also been carried out with similar and consistent results.

Separation angle

Figure 4 shows how the separation angle θ_s (measured from the rear stagnation point) is affected by the buoyancy forces, Gr/Re^2, at $Re = 20$ and $k_s/k_f = \infty$. At $Gr/Re^2 \gtrsim 0.46$ there is no separation region any longer. For negative values of Gr/Re^2, the separation angle is increased and the separated region occupies more and more space and at a certain value of Gr/Re^2, the flow close to the surface is fully recirculating.

At $Re = 40$ and $k_s/k_f = \infty$, the limit of Gr/Re^2 for no separation is ~ 0.84.

Drag coefficient

In Fig. 5, the influence of the buoyancy forces and thermal conductivity ratio on the drag coefficient is shown for $Re = 20$ and $D_c/D = 0.5$ (c_{D_0} is the drag coefficient for $Gr/Re^2 = 0$ and $Re = 20$). For small values of Gr/Re^2, the influence of k_s/k_f is weak but it is increased with increasing values of Gr/Re^2. Again it is found that the buoyancy forces have a stronger effect than the thermal conductivity ratio.

Figure 6 shows some additional results for $Re = 20$ and $D_c/D = 0.11$ but only for positive values of Gr/Re^2. Since the insulator thickness here is greater than for the cases in Fig. 5, the gravity effect is smaller.

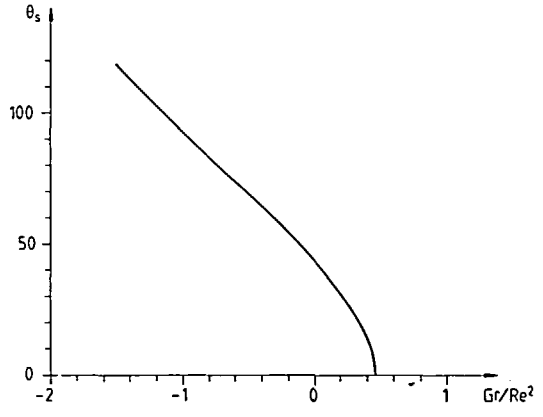

FIG. 4. Separation angle as a function of Gr/Re^2. $Re = 20$ and $k_s/k_f = \infty$.

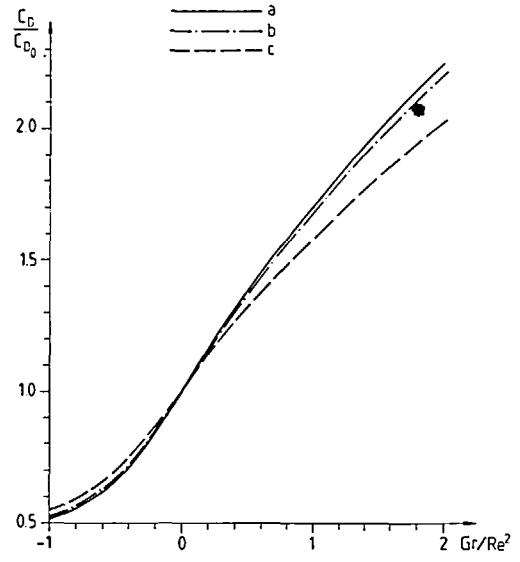

FIG. 5. Influence of the buoyancy forces (Gr/Re^2) and the thermal conductivity ratio (k_s/k_f) on the drag coefficient. $Re = 20$ and $D_c/D = 0.5$. a: $k_s/k_f = 200$, b: $k_s/k_f = 20$, c: $k_s/k_f = 4$.

Figure 7 presents similar results to those in Figs. 5 and 6 but for a Reynolds number of $Re = 40$. Again c_{D_0} is the drag coefficient for $Gr/Re^2 = 0$ and $Re = 40$.

Heat transfer coefficients

In Fig. 8 the influence of the buoyancy forces on the local heat transfer coefficient is shown for $Re = 20$, $D_c/D = 0.5$ and $k_s/k_f = 20$. Curve b is the purely forced flow case. A positive value of Gr/Re^2 increases the local heat transfer over the whole surface probably due to the increased convective transport velocity close to the surface. Negative values of Gr/Re^2 on the other hand decrease the local heat transfer over the major part of the surface. This is so because for negative values of

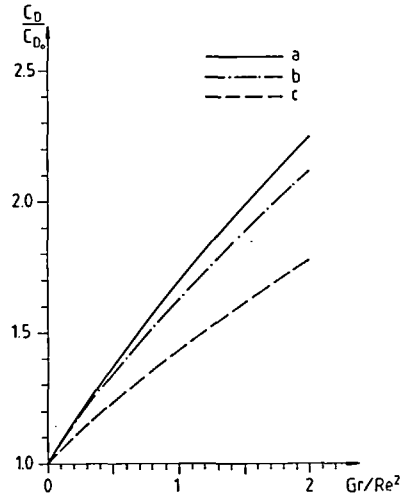

FIG. 6. Influence of the buoyancy forces and the thermal conductivity ratio on the drag coefficient. $Re = 20$ and $D_c/D = 0.11$. a: $k_s/k_f = 200$, b: $k_s/k_f = 20$, c: $k_s/k_f = 4$.

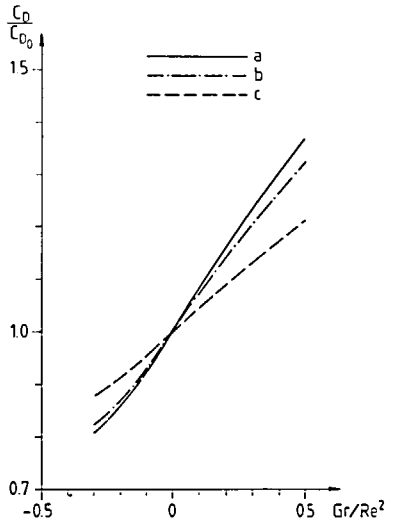

FIG. 7. Influence of the buoyancy forces and the thermal conductivity ratio on the drag coefficient. $Re = 40$ and $D_c/D = 0.11$. a: $k_s/k_f = 200$, b: $k_s/k_f = 20$, c: $k_s/k_f = 4$.

Gr/Re^2, the buoyancy forces counteract the forced flow. However, in the wake region the velocity induced by the buoyancy forces has the same direction as the forced wake velocity and as a result the wake flow becomes more intensive and there is an increase in the local heat transfer.

Figure 9 shows the influence of the buoyancy forces and the thermal conductivity ratio on the mean heat transfer coefficient at $Re = 20$ and $D_c/D = 0.5$. As is evident, the thermal conductivity ratio has a greater effect on the mean heat transfer coefficient than on the drag coefficient (Figs. 5–7).

In Fig. 10 some similar results for $Re = 20$, $D_c/D = 0.11$ and positive values of Gr/Re^2 are given. Since the insulation thickness here is greater than for the cases in Fig. 9, the heat transfer is smaller and the influence of Gr/Re^2 is weaker.

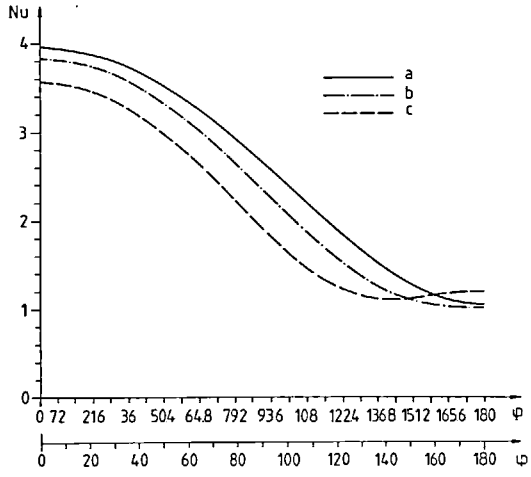

FIG. 8. Influence of the buoyancy forces (Gr/Re^2) on the local heat transfer coefficient. $Re = 20$, $D_c/D = 0.5$ and $k_s/k_f = 20$. a: $Gr/Re^2 = 0.5$, b: $Gr/Re^2 = 0$, c: $Gr/Re^2 = -0.5$.

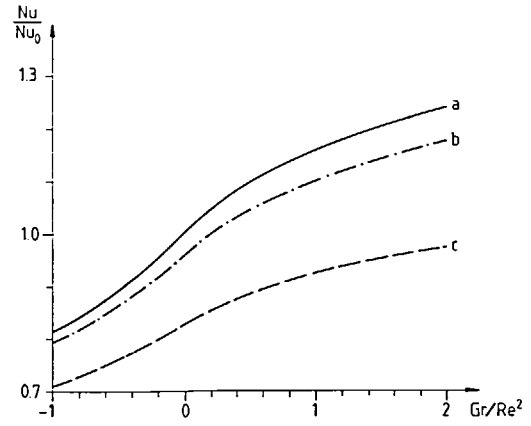

FIG. 9. Influence of the buoyancy forces and the thermal conductivity ratio on the mean heat transfer coefficient. $Re = 20$ and $D_c/D = 0.5$. a: $k_s/k_f = \infty$, b: $k_s/k_f = 20$, c: $k_s/k_f = 4$. Nu_0; forced convection $k_s/k_f = \infty$.

Figure 11 presents results for $Re = 40$ and $D_c/D = 0.11$ which are similar to and consistent with the results given in Figs. 9 and 10.

From the results in Figs. 9–11 it is also clear that with decreasing k_s/k_f the influence of Gr/Re^2 on the mean heat transfer coefficient is diminished.

Correlations of the calculated data

Correlations for determination of the average Nusselt number under combined forced and free convection have been suggested by several authors. So for instance, formulas of the type

$$Nu/Nu_0 = f(Gr/Re^2) \tag{29}$$

where Nu_0 is the Nusselt number for forced convection, have been given by Ousthuizen and Madan [12] and Belyakov *et al.* [37]. Formulas where some form of vectorial addition of the forced and free convection are

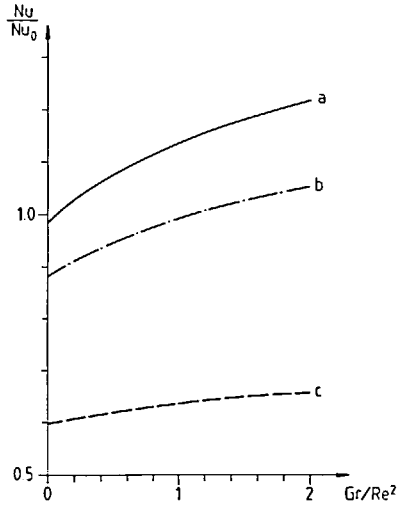

FIG. 10. Influence of the buoyancy forces and the thermal conductivity ratio on the mean heat transfer coefficient. $Re = 20$, $D_c/D = 0.11$. a: $k_s/k_f = 200$, b: $k_s/k_f = 20$, c: $k_s/k_f = 4$.

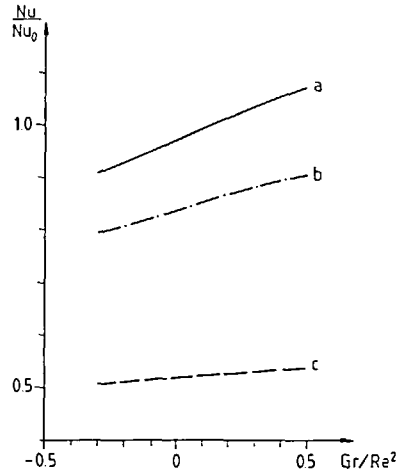

FIG. 11. Influence of the buoyancy forces and the thermal conductivity ratio on the mean heat transfer coefficient. $Re = 40$ and $D_c/D = 0.11$. a: $k_s/k_f = 200$, b: $k_s/k_f = 20$, c: $k_s/k_f = 4$.

used have been presented by for instance Hatton *et al.* [15], van der Hegge Zijnen [18] and Jackson and Yen [38]. Other empirical correlations have also been suggested [16].

In this work, the results for the cases of a uniform surface temperature ($k_s/k_f = \infty$) were correlated to an equation of the form of (29). The reasons for this choice were: (a) the simplicity in the structure of such formulas and (b) it is a convenient formula for engineering calculations. With a least square fit of the calculated data, the following formula was obtained:

$$Nu/Nu_0 = 1 + 0.188(Gr/Re^2) - 0.0126(Gr/Re^2)^2 - 0.011(Gr/Re^2)^3. \quad (30)$$

Also attempts to correlate the calculated data when $k_s/k_f < \infty$ were carried out. However, no simple formula, say $Nu/Nu_0 = \text{function}\,(Gr/Re^2, k_s/k_f, D_c/D)$, could be found to cover all the data. Only for $Gr/Re^2 = 0$ the effect of k_s/k_f could be well described [39].

For the calculated drag coefficients, it was impossible to find a simple formula which could correlate all the data.

5. CONCLUSION

The results of the numerical solutions presented in this paper provide new information concerning flow and heat transfer under influence of buoyancy forces and fluid–solid interactions (coupled solid body heat conduction and convection in a fluid).

The heat transfer has been found to be greatly affected by both the buoyancy forces (Gr/Re^2) and the thermal conductivity ratio (k_s/k_f). For $k_s/k_f = \infty$ a reduction of 18% in the mean heat transfer coefficient occurred at $Gr/Re^2 = -1$ and an increase of 24% was found at $Gr/Re^2 = 2$.

The flow field is primarily affected by the buoyancy forces but also affected by the thermal conductivity ratio when $Gr/Re^2 \neq 0$. For $k_s/k_f = \infty$ the reduction in the drag coefficient is 49% at $Gr/Re^2 = -1$ while at $Gr/Re^2 = 2$ the increase in the drag coefficient is 127%.

Acknowledgements—Financial support from the National Swedish Board for Technical Development (STU) is gratefully acknowledged.

REFERENCES

1. B. Sundén, Conjugated heat transfer from circular cylinders in low Reynolds number flow, *Int. J. Heat Mass Transfer* **23**, 1359–1367 (1980).
2. S. C. R. Dennis, J. D. Hudson and N. Smith, Steady laminar forced convection from a circular cylinder at low Reynolds numbers, *Physics Fluids* **11**, 933–940 (1968).
3. K. M. Krall and E. R. G. Eckert, Heat transfer to a transverse circular cylinder at low Reynolds numbers including rarefaction effects, *Proc. IVth Int. Heat Transfer Conf.*, Vol. III, FC7.5 (1970).
4. P. C. Jain and B. S. Goel, A numerical study of unsteady laminar forced convection from a circular cylinder, *J. Heat Transfer* **98**, 303–307 (1976).
5. D. Sucker and H. Brauer, Stationärer Stoff- und Wärmeübergang an stationär quer angeströmten Zylindern, *Wärme- und Stoffübertragung* **9**, 1–12 (1976).
6. C. J. Apelt and M. A. Ledwich, Heat transfer in transient and unsteady flows past a heated circular cylinder in the range $1 \leqslant R \leqslant 40$, *J. Fluid Mech.* **95**, 761–777 (1979).
7. D. B. Ingham, Free-convection boundary layer on an isothermal horizontal cylinder, *J. Appl. Math. Phys.* **29**, 871–883 (1978).
8. T. H. Kuehn and R. J. Goldstein, Numerical solution to Navier–Stokes equations for laminar natural convection about a horizontal isothermal circular cylinder, *Int. J. Heat Mass Transfer* **23**, 971–979 (1980).
9. S. Nakai and T. Okazaki, Heat transfer from a horizontal circular wire at small Reynolds and Grashof numbers—I, *Int. J. Heat Mass Transfer* **18**, 387–396 (1975).
10. G. A. Öhman, Numerical calculation of steady heat transfer from a horizontal cylinder by combined free and forced convection, *Acta Polytech. Scand. Phys. Incl. Nucl. Ser.* No. 68 (1969).
11. P. C. Jain and B. L. Lohar, Unsteady mixed convection heat transfer from a horizontal circular cylinder, *J. Heat Transfer* **101**, 126–131 (1979).
12. P. H. Ousthuizen and S. Madan, Combined convective heat transfer from horizontal cylinders in air, *J. Heat Transfer* **92**, 194–196 (1970).
13. P. H. Ousthuizen and S. Madan, The effect of flow direction on combined convective heat transfer from cylinders to air, *J. Heat Transfer* **93**, 240–242 (1971).
14. G. K. Sharma and S. P. Sukhatme, Combined free and forced convection heat transfer from a heated tube to transverse air stream, *J. Heat Transfer* **91**, 457–459 (1969).
15. A. P. Hatton, D. D. James and H. W. Swire, Combined forced and natural convection with low-speed air flow over horizontal cylinders, *J. Fluid Mech.* **42**, 17–31 (1970).
16. R. M. Fand and K. K. Keswani, Combined natural and forced convection heat transfer from horizontal cylinders to water, *Int. J. Heat Mass Transfer* **16**, 1175–1191 (1973).
17. B. Gebhart and L. Pera, Mixed convection from long horizontal cylinders, *J. Fluid Mech.* **45**, 49–64 (1971).
18. B. G. van der Hegge Zijnen, Modified correlation formulae for the heat transfers by natural and by forced convection from horizontal cylinders, *Appl. Scient. Res.* **A6**, 129–140 (1956).
19. E. M. Sparrow and L. Lee, Analysis of mixed convection about a horizontal cylinder, *Int. J. Heat Mass Transfer* **19**, 229–231 (1976).
20. J. H. Merkin, Mixed convection from a horizontal circular cylinder, *Int. J. Heat Mass Transfer* **20**, 73–77 (1977).

21. N. D. Joshi and S. P. Sukhatme, An analysis of combined free and forced convection heat transfer from a horizontal circular cylinder to a transverse flow, *J. Heat Transfer* **93**, 441–448 (1971).
22. A. Mocoglu and T. S. Chen, Analysis of combined forced and free convection across a horizontal cylinder, *Can. J. Chem. Engng* **55**, 265–271 (1977).
23. V. T. Morgan, The overall convective heat transfer from smooth circular cylinders, *Adv. Heat Transfer* **11**, 199–264 (1975).
24. B. Sundén, A coupled conduction-convection problem at low Reynolds number flow, in *Numerical Methods in Thermal Problems I*, pp. 412–422. Pineridge Press Swansea, Wales (1979).
25. B. Sundén, A coupled conduction-convection study in the slip-flow regime, in *Numerical Methods in Thermal Problems II*, pp. 1084–1095. Pineridge Press Swansea, Wales (1981).
26. B. Sundén, A numerical study of coupled conduction-mixed convection, in *Numerical Methods for Non-Linear Problems*, pp. 795–805. Pineridge Press Swansea, Wales (1980).
27. E. R. G. Eckert and E. Soehngen, Distribution of heat transfer coefficients around circular cylinders in cross flow at Reynolds numbers from 20 to 500, *Trans. Am. Soc. Mech. Engrs* **74**, 343–347 (1952).
28. M. Coutanceau and R. Bouard, Experimental determination of the main features of the viscous flow in the wake of a circular cylinder in uniform translation, *J. Fluid Mech.* **79**, 231–256 (1977).
29. I. Imai, On the asymptotic behaviour of viscous fluid flow at a great distance from a cylindrical body with special reference to Filon's paradox, *Proc. R. Soc.* **A208**, 487–516 (1951).
30. H. B. Keller and H. Takami, Numerical studies of steady viscous flow about cylinders, *Proc. Symp. on Numerical Methods of Nonlinear Differential Equations*, Univ. of Wisconsin (1966).
31. H. Takami and H. B. Keller, Steady two-dimensional viscous flow of an incompressible fluid past a circular cylinder, *Physics Fluids Suppl.* **2**, II-51–II-56 (1969).
32. Y. Takaisi, Numerical studies of a viscous liquid past a circular cylinder, *Physics Fluids Suppl.* **2**, II-86–II-87 (1969).
33. M. Kawaguti, Numerical solution of Navier–Stokes' equations for the flow around a circular cylinder at Reynolds number 40, *J. Phys. Soc. Japan* **8**, 747–757 (1953).
34. F. Nieuwstadt and H. B. Keller, Viscous flow past circular cylinders, *Comp. Fluids* **1**, 59–71 (1973).
35. B. Fornberg, A numerical study of steady viscous flow past a circular cylinder, *J. Fluid Mech.* **98**, 819–855 (1980).
36. S. C. R. Dennis; A numerical method for calculating steady flow past a cylinder, *Proc. 5th Int. Conf. Numerical Methods in Fluid Dynamics*, pp. 165–172 (1976).
37. V. A. Belyakov, P. M. Brdlik and Yu. P. Semenov, Experimental investigation of mixed air convection near a horizontal cylinder, *J. Appl. Mech. Tech. Phys.* **21**, 228–232 (1980).
38. T. W. Jackson and H. H. Yen, Combining forced and free convection equations to represent combined heat transfer coefficients for a horizontal cylinder, *J. Heat Transfer* **93**, 247–248 (1971).
39. B. Sundén, Conjugated heat transfer at low Reynolds number flow around a circular cylinder, Publ. No. 78/5, Dept. of Appl. Thermo and Fluid Dynamics, Chalmers Univ. of Techn., Göteborg (1978).

INFLUENCE DES FORCES D'ARCHIMEDE ET DE LA CONDUCTIVITE THERMIQUE SUR LE CHAMP DE VITESSE ET SUR LE TRANSFERT THERMIQUE DES CYLINDRES CIRCULAIRES AUX FAIBLES NOMBRES DE REYNOLDS

Résumé—On présente une étude numérique de l'influence des forces d'Archimède et du rapport de conductivité thermique (k_s/k_f) sur le champ d'écoulement et sur le transfert thermique autour de cylindres circulaires. Le champ de vitesse et les équations d'énergie sont résolus sous les conditions de continuité de température et de flux thermique à l'interface fluide–solide. Les forces d'Archimède sont prises en compte en appliquant l'approximation de Boussinesq. Des résultats numériques sont donnés pour le nombre de Reynolds dans le domaine $5 \leqslant Re \leqslant 40$, le paramère mixte dans le domaine $-1 \leqslant Gr/Re^2 \leqslant 2$ et le rapport de conductivités dans le domaine $0 \leqslant k_s/k_f \leqslant \infty$.

EINFLUSS VON AUFTRIEBSKRÄFTEN UND WÄRMELEITUNG AUF DAS STRÖMUNGSFELD UND DEN WÄRMETRANSPORT AN KREISZYLINDERN FÜR KLEINE REYNOLDS-ZAHLEN

Zusammenfassung—Der Einfluß der Auftriebskräfte und des Verhältnisses der Wärmeleitfähigkeiten (k_s/k_f) auf das Strömungsfeld und den Wärmetransport an Kreiszylindern wurde untersucht. Die Bewegungs- und Energiegleichungen werden unter der Bedingung stetigen Temperatur- und Wärmestromverlaufs an der Grenzfläche zwischen Zylinder und Flüssigkeit gelöst. Die Auftriebskräfte werden durch Anwendung der Boussinesq-Approximation berücksichtigt. Die numerischen Ergebnisse werden für Reynolds-Zahlen im Bereich von $5 \leqslant Re \leqslant 40$, die für Auftriebsparameter im Bereich von $-1 \leqslant Gr/Re^2 \leqslant 2$ und für Verhältnisse der Wärmeleitfähigkeiten im Bereich von $0 \leqslant k_s/k_f \leqslant \infty$ angegeben.

ВЛИЯНИЕ ПОДЪЕМНЫХ СИЛ И ТЕПЛОПРОВОДНОСТИ НА ПОЛЕ ТЕЧЕНИЯ И ТЕПЛОПЕРЕНОС В КОЛЬЦЕВЫХ ЦИЛИНДРАХ ПРИ МАЛЫХ ЧИСЛАХ РЕЙНОЛЬДСА

Аннотация—Представлено численное исследование влияния подъемных сил и отношения теплопроводностей (k_s/k_f) на поле течения и теплоперенос вокруг кольцевых цилиндров. Уравнения гидродинамики и энергии решаются в предположении непрерывности температуры и теплового потока на границе раздела жидкость-твердое тело. Подъемные силы учитываются в приближении Буссинеска. Численные результаты приведены для значения числа Рейнольдса в диапазоне $5 \leq Re \leq 40$, параметра подъемных сил в диапазоне $-1 \leq Gr/Re^2 \leq 2$ и отношения теплопроводностей в диапазоне $0 \leq k_s/k_f \leq \infty$.